# Development of Proton Conducting Electrolytes with Enhanced Performance and Stability for Reversible Solid Oxide Cells

Zheyu Luo, Yucun Zhou, Xueyu Hu, and Meilin Liu

School of Materials Science & Engineering, Georgia Tech, Atlanta, GA 30332-0245

## Introduction

- Reversible solid oxide cells based on proton conductors have potential to be the most efficient and low-cost option for energy storage and power generation, holding promise as an enabler for the implementation of intermittent renewable energy technologies and the widespread utilization of hydrogen.
- Acceptor-doped barium cerate-based proton conductors have the highest ionic conductivity at intermediate temperatures.
- While highly conductive, some doped barium cerates are unstable against high concentrations of $H_2O/CO_2$. It's necessary to investigate the effect of more dopants on enhancing chemical stability while retaining high conductivity.

## Results and Discussion

### 1. Conductivity and ionic transference number

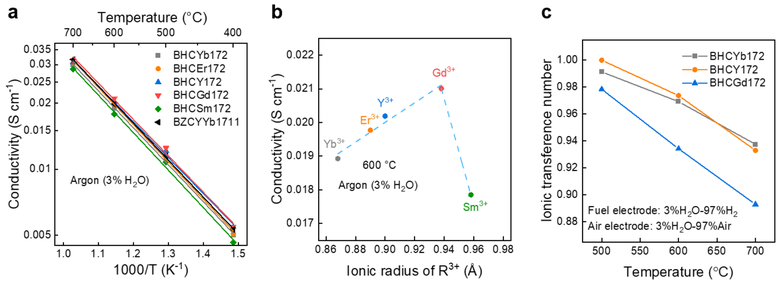


**Figure 1. a)** Conductivity of BHCR172 (R = Yb, Er, Y, Gd, Sm) and BZCYYb1711 as a function of temperature. **b)** Conductivity of BHCR172 at 600 °C as a function of ionic radius of $R^{3+}$. **c)** Ionic transference number measured under cell operation conditions.

### 2. Chemical stability against $H_2O$ and $CO_2$

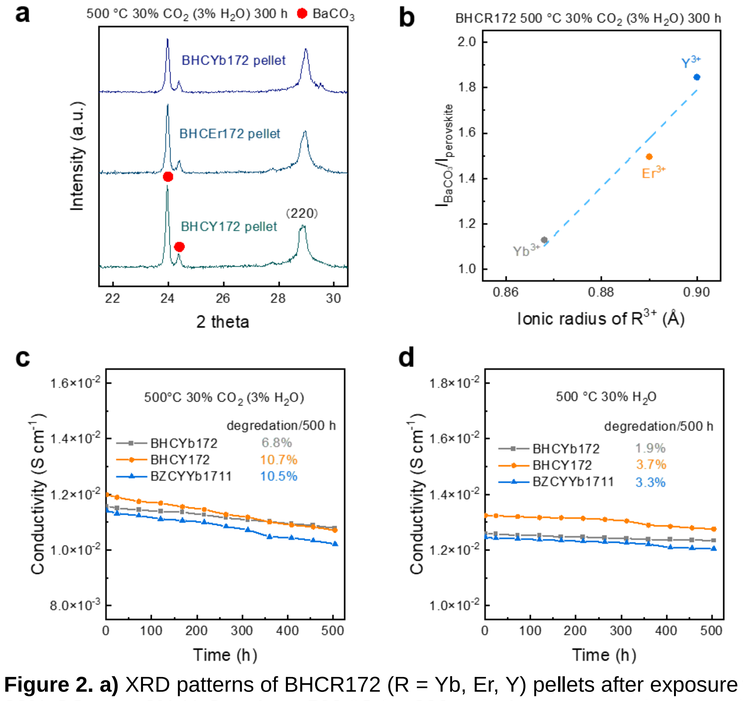


**Figure 2. a)** XRD patterns of BHCR172 (R = Yb, Er, Y) pellets after exposure to 30% $CO_2$ and 3% $H_2O$ in Ar at 500 °C for 300 h. **b)** Intensity ratio between the $BaCO_3$ and perovskite (220) peaks of BHCR172 as a function of ionic radius of $R^{3+}$. Conductivity of BHCYb172, BHCY172, and BZCYYb1711 over 500 h in **c)** 30% $CO_2$ and 3% $H_2O$, and **d)** 30% $H_2O$ in Ar at 500 °C.

### 3. DFT-based calculations

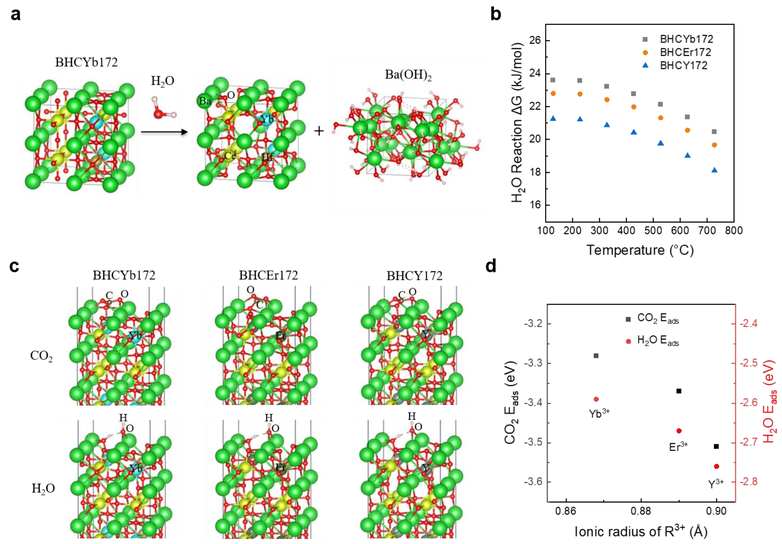


**Figure 3. a)** The $H_2O$ reaction schematic between BHCYb172 and $H_2O$. **b)** Gibbs free energy curves for the reaction of $H_2O$ with BHCR172 (R=Yb, Er, Y). **c)** The $CO_2$ (top) and $H_2O$ (bottom) adsorption behavior for AO-terminated BHCR172 (001) surfaces. **d)** $CO_2$ and $H_2O$ $E_{ads}$ as a function of the ionic radius of $R^{3+}$.

### 4. Compatibility with Ni-based electrodes

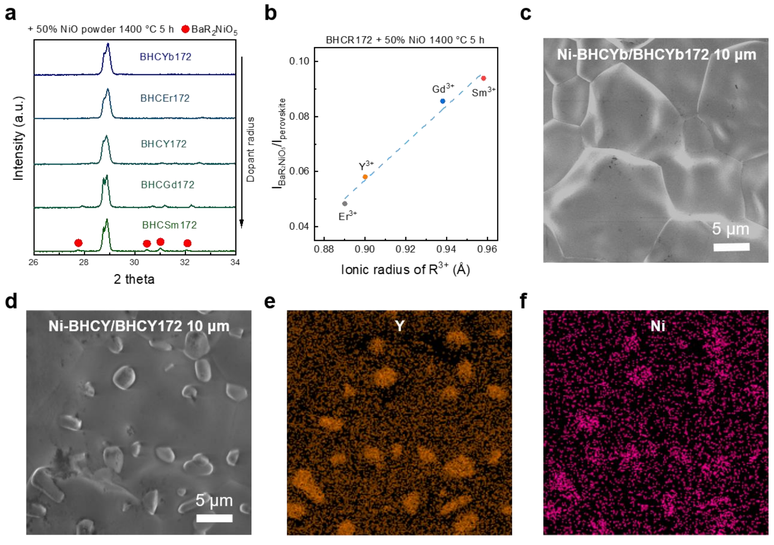


**Figure 4. a)** Magnified view of XRD patterns of BHCR172 (R = Yb, Er, Y, Gd, Sm) after firing with NiO at 1400 °C for 5 h. **b)** Intensity ratio between the $BaR_2NiO_5$ and perovskite (220) peaks of BHCR172 (R = Er, Y, Gd, Sm) as a function of the ionic radius of $R^{3+}$. **c)** SEM image of the electrolyte surface of a Ni-BHCYb/BHCYb172 half cell with an electrolyte thickness of 10 μm after firing at 1400 °C for 5 h. **d-f)** SEM image and EDS mapping of the electrolyte surface of a Ni-BHCY/BHCY172 half cell with an electrolyte thickness of 10 μm after firing at 1400 °C for 5 h.

Luo, Z., Zhou, Y., Hu, X., Kane, N., Li, T., Zhang, W., Liu, Z., Ding, Y., Liu, Y., & Liu, M. (2022). *Energy & Environmental Science, 15*, 2992-3003

### 5. Impact of NiO compatibility on cell performance

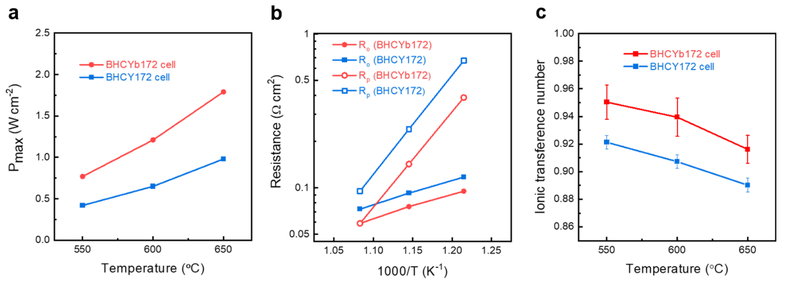


**Figure 5.** Comparison of **a)** peak power density, **b)** ohmic and polarization resistance, and **c)** ionic transference number between BHCYb172- and BHCY172-based single cells.

### 6. Electrochemical performance of BHCYb172-based single cells

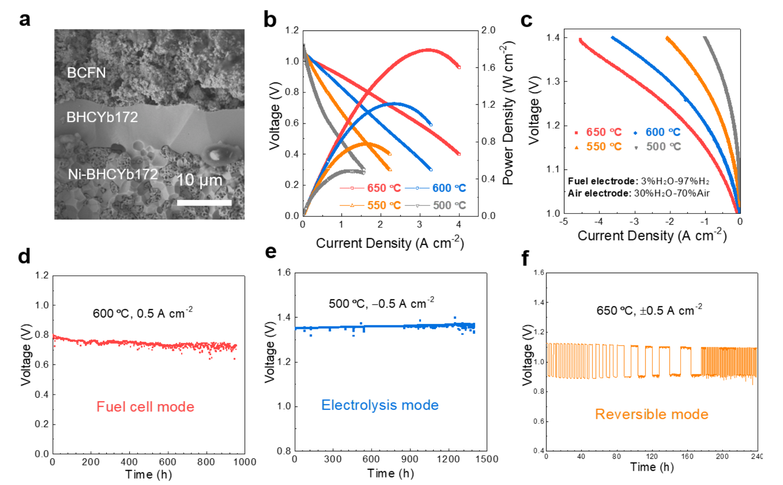


**Figure 6. a)** Cross-sectional SEM image of the Ni-BHCYb172/BHCYb172/BCFN single cell. **b)** Typical I-V-P curves measured in the fuel cell mode at 500-650 °C with $H_2$ (3% $H_2O$) in the fuel electrode and ambient air in the air electrode. **c)** Typical I-V curves measured in the electrolysis mode at 500-650 °C with $H_2$ (3% $H_2O$) in the fuel electrode and air (30% $H_2O$) in the air electrode. **d)** Long-term stability in the fuel cell mode with $H_2$ (3% $H_2O$) in the fuel electrode and ambient air in the air electrode at 0.5 A cm$^{-2}$ and 600 °C. **e)** Long-term stability in the electrolysis mode with $H_2$ (3% $H_2O$) in the fuel electrode and air (3% $H_2O$) in the air electrode at -0.5 A cm$^{-2}$ and 500 °C. **f)** Reversible operation of the cell: the cell voltage as a function of time when the operating mode was switched between the fuel cell and electrolysis modes (2-12 h for each mode) at a current density of ±0.5 A cm$^{-2}$ at 650 °C.

## Summary

- Developed a Yb-doped proton conductor with enhanced stability and minimal reaction towards NiO
- Conductivity, stability, and NiO compatibility are all closely correlated with the acceptor dopant size
- Demonstrated high-performance solid oxide cells based on novel BHCYb172 proton conducting electrolyte

## Acknowledgement

This work was supported by US Department of Energy, Office of Fossil Energy, Small-Scale Solid Oxide Fuel Cell Systems and Hybrid Electrolyzer Technology Development Program under the Award Number DE-FE0031975 and Phillips 66.